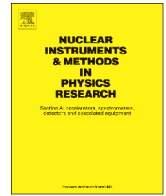




ELSEVIER

Contents lists available at ScienceDirect

# Nuclear Instruments and Methods in Physics Research A

journal homepage: [www.elsevier.com/locate/nima](http://www.elsevier.com/locate/nima)

## Study of the readout configuration of the GAMMA-400 silicon tracker sensors

A. Berra<sup>a,b,\*</sup>, V. Bonvicini<sup>c</sup>, D. Lietti<sup>a,b</sup>, M. Prest<sup>a,b</sup>, E. Vallazza<sup>c</sup><sup>a</sup> Università degli Studi dell'Insubria, Via Valleggio, 11 - 22100 Como, Italy<sup>b</sup> INFN sezione di Milano Bicocca, Piazza della Scienza, 3 - 20126 Milano, Italy<sup>c</sup> INFN sezione di Trieste, Via Valerio, 2 - 34127 Trieste, Italy

### ARTICLE INFO

#### Article history:

Received 22 June 2015

Received in revised form

10 July 2015

Accepted 11 July 2015

Available online 23 July 2015

#### Keywords:

Silicon Strip Tracker

GAMMA-400

Gamma Rays

Cosmic Rays

### ABSTRACT

The GAMMA-400 satellite is an upcoming international space mission designed to detect gamma and cosmic rays in a broad energy range up to 3 TeV, with an excellent angular and energy resolution. The present design foresees a 10 layers Si–W tracker formed by single sided silicon sensors with 80 μm strip pitch, with a readout pitch of 240 μm; the sensors are arranged in four towers, each one with an area of 50 × 50 cm<sup>2</sup>, for a total of more than 150k channels. This paper presents an analysis of the spatial resolution of the proposed readout configuration, compared with different readout approaches, both in terms of readout pitch and strip/implant widths. The study has been performed with two specially developed silicon modules, each one divided into zones with different characteristics. The tests have been performed on the CERN PS-T9 beamline using 10 GeV negative particles.

© 2015 Elsevier B.V. All rights reserved.

### 1. Introduction

The GAMMA-400 (Gamma Astronomical Multifunctional Modular Apparatus) space observatory is a space mission approved by the Russian Space Agency to investigate many important aspects in the gamma ray astronomy and in cosmic ray science [1]. The main goals of the mission are

- the study of gamma rays in the 100 MeV–3 TeV energy range;
- the study of high energy electrons/positrons up to the TeV region;
- the search for Dark Matter candidates;
- the study of the acceleration mechanism of galactic and extragalactic cosmic rays.

The converter–tracker system of GAMMA-400 consists of 10 double layers of microstrip silicon detectors, interleaved with thin (0.08 X<sub>0</sub>) tungsten layers. The system is used to pair-convert the photons and to precisely reconstruct the photon direction by the precise detection in the silicon layers of the e<sup>+</sup>–e<sup>–</sup> pair tracks. For more details on the GAMMA-400 converter–tracker see [1,2]. The present design of the silicon microstrip sensors foresees single sided devices with an implant pitch of 80 μm and a readout pitch

of 240 μm, using the capacitive charge division approach [3]. Considering the large dimensions of the complete silicon tracker (four towers with an area of 50 × 50 cm<sup>2</sup> each), this readout scheme was chosen in order to reduce as much as possible the number of electronic channels, still maintaining a good spatial resolution. In this configuration, the Si–W tracker features 153,600 readout channels: thanks to the use of low-power ASICs (see Section 2), the total power consumption of the tracker front-end electronics is approximately 80 W [1].

The goal of this paper is to compare the spatial resolution of the selected readout approach with respect to other possible layouts of the sensors. The first two sections of this paper are devoted to the description of the GAMMA-400 prototype silicon sensors, characterized by different zones with different implant widths and readout schemes, and of the experimental setup used to characterize the prototype; the last section presents the results obtained in a particle beamtest performed at the CERN PS-T9 beamline in September 2014.

### 2. The GAMMA-400 prototype silicon sensors

The prototype silicon sensors used in this study were fabricated by FBK, Trento, Italy [4], on high-resistivity, high-purity n-type silicon wafers of 6 in. diameter. The detectors have a dimension of 53.16 × 32.76 mm<sup>2</sup> and a thickness of 300 μm. Two sensor layouts have been designed: the first one has 384 p<sup>+</sup> strip implants with a

\* Corresponding author at: Università degli Studi dell'Insubria, Via Valleggio, 11 - 22100 Como, Italy.

E-mail address: [alessandro.berra@gmail.com](mailto:alessandro.berra@gmail.com) (A. Berra).

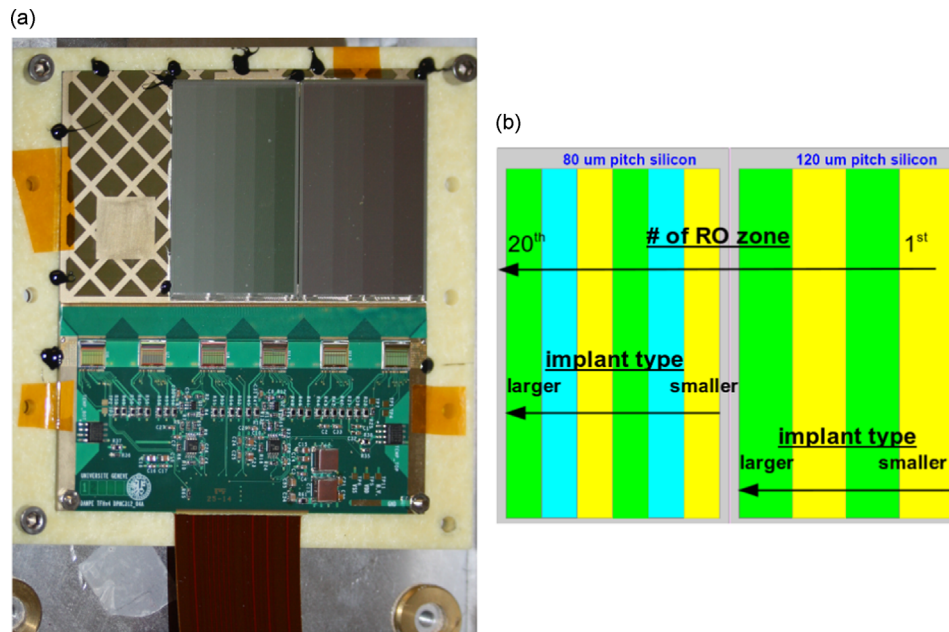


**Fig. 1.** Picture (a) and sketch (b) of the strip layout of the two GAMMA-400 silicon sensors. In (a) also the ASICs and the hybrid support can be seen: the strip/ASICs bonding procedure has been performed at INFN-Perugia.

pitch of 80  $\mu\text{m}$ , the second one has 256  $\text{p}^+$  strip implants with a pitch of 120  $\mu\text{m}$ . In both designs, the strips are AC-coupled via integrated coupling capacitors and the DC-bias of the strips is achieved by punch-through. Each sensor is divided into different zones, characterized by different pitches and different implant widths: in the 80  $\mu\text{m}$  pitch design there are 6 groups (each one comprising 64 strips) with implant widths of 20, 30, 40, 50, 55 and 60  $\mu\text{m}$ ; in the 120  $\mu\text{m}$  pitch design there are 4 groups (64 strips each) with implant widths of 30, 40, 50 and 60  $\mu\text{m}$ . Fig. 1b presents a simplified sketch of the strip layout of the two sensors, while Table 1 summarizes the characteristics of each sensor zone and reports the readout pitch used in the test for the different zones.

The two silicon sensors are readout by five high dynamic range (200 fC) VA-140 64 channels ASICs (Gamma Medica-IDEAS, Norway) built in 0.35  $\mu\text{m}$  CMOS technology [5]. Each channel consists of

- a low-noise (425  $\text{e}^-$  RMS) and low power (0.29 mW) charge sensitive preamplifier;
- a CR-RC shaper;
- a sample & hold circuit (peaking time of 6.5  $\mu\text{s}$ ).

### 3. Experimental setup and DAQ

The GAMMA-400 prototypes were tested on the PS-T9 beam-line, using negative particles (mainly muons and pions) with an energy of 10 GeV: the focusing of the beam optics was set in order to have a parallel beam. The detectors were placed inside an aluminum frame, which protects the silicon sensors and holds the front-end electronics: the frame can be also interfaced with a tiltable support, allowing us to measure the spatial resolution for different angles of the impinging particles (Fig. 2). The tilt angle can be selected in steps of 15°, inserting a calibrated metal pin in a drilled wheel.

The experimental setup can be divided into two parts: the tracking system and the trigger system. The tracking system is based on a pair of silicon beam telescopes, originally developed by INFN-Trieste [6]. Each telescope consists of a double sided silicon

**Table 1**  
Characteristics of each silicon sensor zone.

Zone	Physical strip pitch ( $\mu\text{m}$ )	Readout pitch ( $\mu\text{m}$ )	Implant width ( $\mu\text{m}$ )	# of ASIC channels
1	120	120	30	18
2	120	240	30	16
3	120	240	40	17
4	120	120	40	15
5	120	120	50	17
6	120	240	50	14
7	120	240	60	16
8	120	120	60	17
9	80	160	20	14
10	80	240	20	10
11	80	240	30	10
12	80	160	30	10
13	80	160	40	11
14	80	240	40	12
15	80	240	50	9
16	80	160	50	13
17	80	160	55	10
18	80	240	55	10
19	80	240	60	9
20	80	160	60	19

strip detector ( $1.92 \times 1.92 \text{ cm}^2$ , 300  $\mu\text{m}$  thick) manufactured by CSEM<sup>1</sup> and its front-end electronics. The p-side of the detector has a  $\text{p}^+$  implantation strip every 25  $\mu\text{m}$  and a readout pitch of 50  $\mu\text{m}$  while the n-side (which is perpendicular to the p-one) has  $\text{n}^+$  implantation strips with a pitch of 50  $\mu\text{m}$ , separated by  $\text{p}^+$  blocking strips. Each silicon side is readout by three VA2 128 channel ASICs, built with a 1.2  $\mu\text{m}$  N-well CMOS technology. Each ASIC channel consists of [7]

- a low-noise (80  $\text{e}^-$  RMS) low power (1.3 mW) charge sensitive preamplifier;

<sup>1</sup> Centre Suisse d'Electronique et de Microtechnique SA, CH, <http://www.csem.ch/site/>

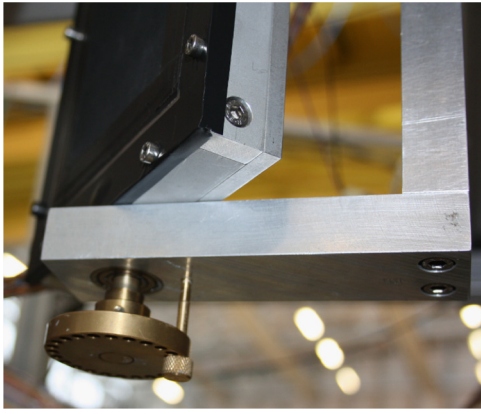


**Fig. 2.** The drilled wheel used to tilt the frame, with the calibrated metal pin in position.

- a CR-RC shaper;
- a sample & hold circuit (peaking time selectable between 1–3  $\mu$ s).

The 128 output signals are multiplexed onto a single output line with a maximum frequency for the readout clock of 10 MHz. The three ASICs are AC coupled to the double sided detectors (Fig. 3b) via external quartz capacitors and are interfaced with the rest of the front-end electronics with a multi-layer ceramic hybrid. The spatial resolution of the p-side, measured with a 150 GeV/c electron beam, is equal to  $\sim 4 \mu\text{m}$  [7]. A picture of the setup is presented in Fig. 3a: since the p-sides of the beam telescopes are characterized by a better spatial resolution, the GAMMA-400 module was placed with the strips oriented in the same direction.

The trigger system consists of two scintillator counters: the first one is positioned directly at the end of the beamline, while the second, characterized by smaller dimensions ( $3 \times 4 \text{ cm}^2$  with respect to  $10 \times 10 \text{ cm}^2$ ), is directly mounted on the first silicon telescope by means of a dedicated support (Fig. 4).

The DAQ is a standard VME system controlled by a SBS Bit3 model 620 bridge<sup>2</sup>, optically linked to a Linux PC-system. A dedicated VME board (the trigger board) is responsible for the conditioning of the trigger, processing both the scintillators and the spill signals. The trigger signal is then sent to three VME VRB boards [8] (designed by INFN-Trieste) to generate the DAQ trigger and the readout sequence of the silicon detectors. The VRB hosts an Altera EP2C50 FPGA with 50k cells and 581 kbit of internal RAM (which allows also to check complex designs with the embedded logic state analyzer) and 4 PLLs (Phase Locked Loop) for the clock generation. The board has 16 LVDS (Low-Voltage Differential Signaling) inputs and 16 LVDS outputs, 2 TTL inputs and 2 TTL outputs, a TLK1501 Gigabit link and 4 Mword of 32 bit RAM. When the VRB receives the data, the input from each board is de-multiplexed and each stream of data is copied in the RAM, and transferred to the PC during the interspill period. The VRB boards are also responsible for the ASICs configuration before the start of the run. The signals of both the silicon beam telescopes and of the GAMMA-400 prototype are digitized by three dedicated ADC boards and sent back to the control boards.

#### 4. Silicon sensors analysis

Considering the difference in lateral dimensions between the beam telescopes (less than 2 cm) and the complete GAMMA-400

module ( $\sim 6.5 \text{ cm}$ ), different runs have been acquired, shifting each time the position of the GAMMA-400 frame, in order to scan different zones on the module: for each position, five tilt angle configurations ( $0^\circ$  and  $60^\circ$ ) were tested. The analysis procedure can be divided into three steps:

- analysis of the pedestals of each silicon detector;
- definition of the thresholds and selection of the good events;
- spatial resolution analysis using the residuals method.

##### 4.1. Pedestal analysis

To evaluate the pedestal and the noise of each channel, a pedestal run of 200 events was acquired with a random trigger. The mean value of each channel represents the pedestal while the RMS corresponds to the noise. Fig. 5 presents an example of the pedestal of one silicon module.

The black histogram in the bottom part of Fig. 5b is the global noise RMS while the red one is the noise RMS after the common mode<sup>3</sup> subtraction. The common mode for each ASIC was computed on an event by event basis as

$$\sum_{j=1}^{n_{\text{ASIC}}} CM_j = \sum_{j=1}^{n_{\text{ASIC}}} \frac{\sum_{i=1}^{n_{\text{Strip}}} (\text{raw}_i - \text{pede}_i)}{N_j} \quad (1)$$

where  $j$  represents the number of the ASIC and runs over the total number of ASICs, while  $i$  is the number of channels for each ASIC and may run over the total number of ASIC channels. The mean value ( $CM_j$ ) was computed excluding the dead or noisy channels ( $N$  represents the number of good channels). The RMS noise  $CM$  subtracted is used in the analysis as a reference for the threshold definition.

##### 4.2. Event selection

The event selection was performed by means of the *pull* variable, defined as the ratio between the pulse height (that is the particle signal which is obtained subtracting from the raw data the pedestal value) of the strip with the maximum signal in the event and its corresponding noise RMS. The pull distributions for the strips with the maximum signal for the GAMMA-400 module are presented in Fig. 6.

Fig. 6 presents a dual peak distribution, where each peak corresponds to a specific detector zone (in this particular case, the peak at  $\sim 10$  corresponds to the  $240 \mu\text{m}$  readout zone, while the peak at  $\sim 20$  corresponds to the  $160 \mu\text{m}$  readout zone). The dashed line in Fig. 6 represents the selected thresholds to detect a particle event (corresponding to a pull value of 7).

The exact position of the particle in the detector was computed by means of a cluster-finding algorithm, characterized by different steps:

- the evaluation of the strips above a certain threshold, chosen according to the pull variable distribution ( $20\sigma$  for the beam telescopes,  $7\sigma$  for the GAMMA-400 module);
- the cluster identification, performed taking into account the lateral strips that surround the one with the maximum signal: these strips were selected choosing a lower threshold for their signals ( $10\sigma$  for the beam telescopes,  $4\sigma$  for the GAMMA-400 module);
- the evaluation of the cluster position by means of the center of gravity method; the position of the cluster was computed as

<sup>3</sup> The common mode noise is the noise contribution due to the external noise on the detector bias line (for example the electromagnetic noise). It causes a common variation of the baseline of all the strips on an event by event basis.

<sup>2</sup> SBS Technologies Inc., USA, <http://www.ge-ip.com>

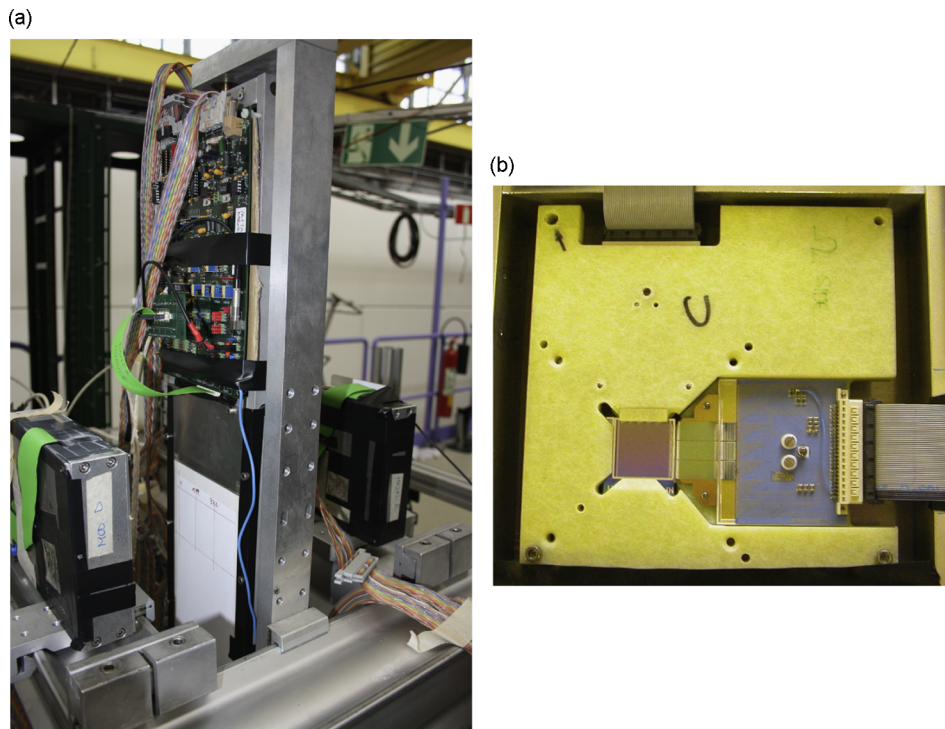


**Fig. 3.** The GAMMA-400 module between the two silicon telescopes (a); a detail of the silicon beam telescope with the three VA2 ASICs connected to the ohmic side of the tile (b).

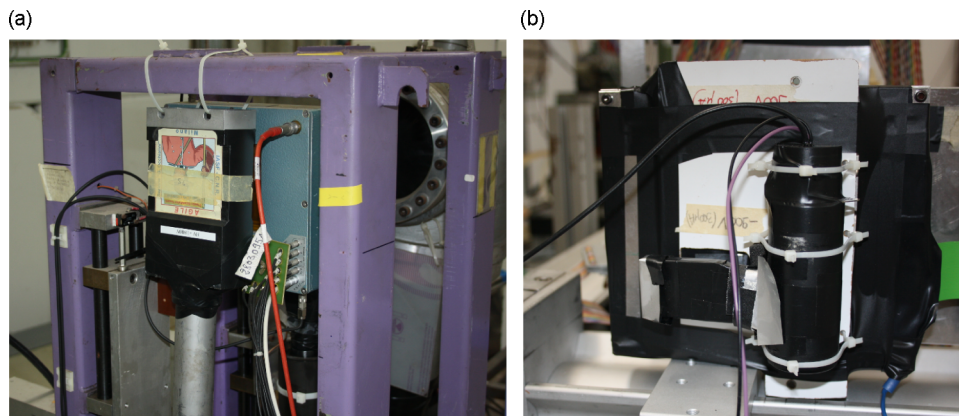


**Fig. 4.** Picture of the large (a) and small (b) scintillator counters used for the trigger system.

$xPos = \frac{\sum_i x_i PH_i}{\sum_i PH_i}$  where the  $i$  index runs over the number of strips that compose the cluster,  $x_i$  is the position of the  $i$ th strip of the cluster and  $PH_i$  is the pulse height of that strip.

Others and more reliable cluster position finding algorithms could be used: for example, the  $\eta$  algorithm should provide a slightly more accurate cluster position reconstruction [9]. However, the  $\eta$  algorithm has two main drawbacks:

- it can be used only with clusters composed of two or more strips, while the center of gravity method can be used with clusters formed by any number of strips;
- it is less precise than the standard center of gravity algorithm for strongly inclined tracks.

The final event selection was performed considering the distribution of the number of clusters per event (Fig. 7), selecting

only the single cluster events (considering that only two beam telescopes were used, a particle could be tracked without ambiguity only if one single cluster was present in each detector). The large number of “zero” cluster events that can be seen in Fig. 7a is due to the fact that both trigger scintillators were larger than the beam telescope dimensions, thus the DAQ was triggered even if no particles crossed the sensitive area of the telescopes.

#### 4.3. Resolution analysis

The beam profiles reconstructed with the first beam telescope and with the GAMMA-400 module are presented in Fig. 8. The parallel setting of the beam focusing resulted in a very broad beam shape, which covered a large part of the GAMMA-400 module. In particular, Fig. 8b clearly shows the different zones of the silicon detector, separated by strips not connected to the

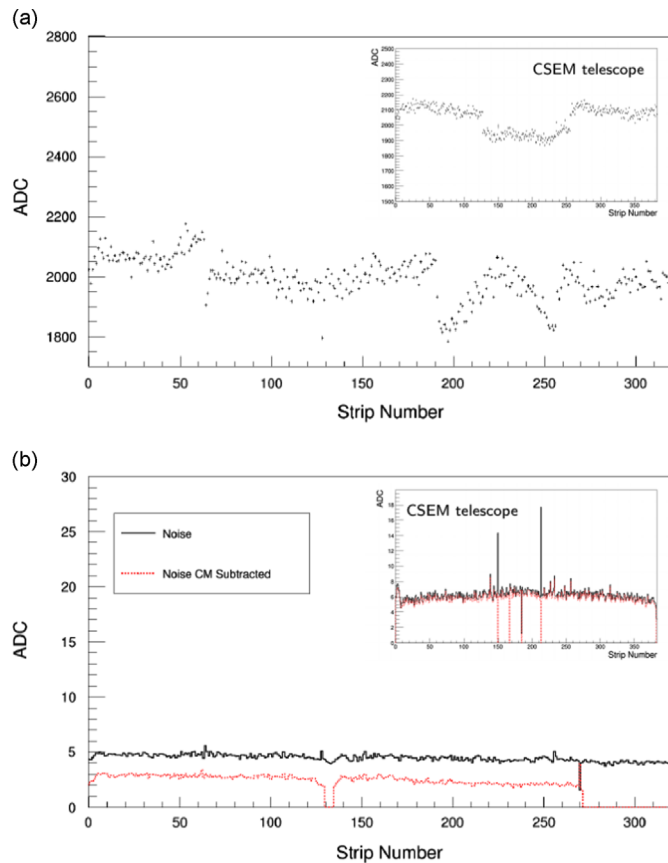


**Fig. 5.** Example of pedestal profile histogram (a) and extracted RMS noise distributions (b) for the GAMMA-400 module. The small embedded pictures refer to one of the beam telescope modules. (For interpretation of the references to color in this figure, the reader is referred to the web version of this paper.)

ASICs. The beam divergence was of the order of 1.6 mrad in the horizontal direction (Fig. 8c).

The spatial resolution of the GAMMA-400 module was computed with the residual method: the residual is defined as the difference between the real particle impact point (obtained reconstructing the particle trajectory with the beam telescopes and projecting this trajectory on the GAMMA-400 module) and the reconstructed position (obtained with the position finding algorithm). The spatial resolution of the detectors is defined as the RMS of the distribution of the residuals and corresponds to the uncertainty in the reconstructed coordinates. Considering the number of zones of the GAMMA-400 module, a residual plot was computed for each zone: an event is assigned to a zone if the reconstructed position of the cluster matches the zone position in the strips map (Table 1). An example of a residual distribution is presented in Fig. 9a. To compute the spatial resolution, the residual distributions were fitted with a composite function, formed combining a Gaussian function, used to model the main peak, with an asymmetric Gaussian, which handles the distribution tails (Fig. 9b). The fitting procedure was performed with the RooFit package of the CERN ROOT data analysis framework<sup>4</sup>.

Fig. 10 presents the comparison between the different readout approaches, obtained with perpendicular impinging

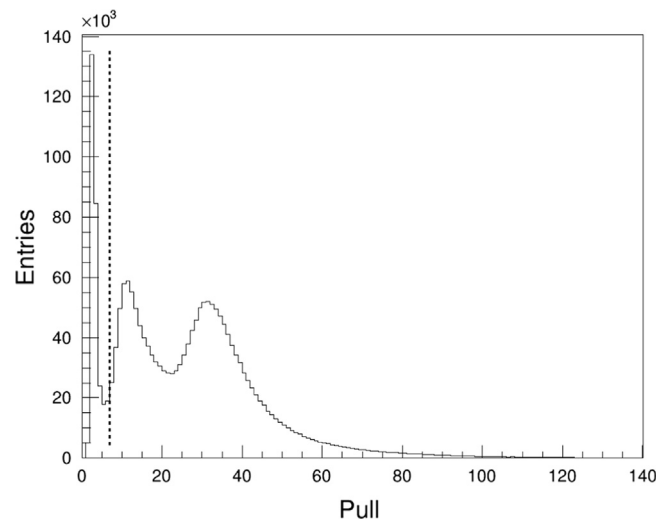


**Fig. 6.** Example of pull distribution for the GAMMA-400 module.

particles, varying the implant width. The following considerations hold:

- the zones with a smaller strip pitch are characterized by a better spatial resolution:  $\sim 30 \mu\text{m}$  for the  $80 \mu\text{m}$  pitch with respect to  $\sim 40 \mu\text{m}$  for the  $120 \mu\text{m}$  pitch;
- the spatial resolution improves increasing the implant width, due to a better charge collection: however, this effect is more evident within the  $80 \mu\text{m}$  pitch zones;
- thanks to the capacitive coupling, the spatial resolutions of the  $80 \mu\text{m}$  pitch zones with  $160$  or  $240 \mu\text{m}$  readout pitch are quite similar, with a difference of the order of  $2\text{--}3 \mu\text{m}$ : in particular, the difference is almost irrelevant when an implant larger than  $50 \mu\text{m}$  is used;
- the resolution obtained in the  $80 \mu\text{m}$  strip,  $160 \mu\text{m}$  readout pitch zone with the  $60 \mu\text{m}$  implant is slightly larger than the previous configurations: this is somehow unexpected, considering the trend obtained with the smaller implant widths (up to  $55 \mu\text{m}$ ) and the fact that at larger implant widths corresponds a better charge collection. This is possibly due to the fact that this is the last zone of the GAMMA-400 silicon sensor, and thus was poorly illuminated by the particle beam (less than  $1\text{k}$  events after the selection cuts, compared to more than  $\sim 15\text{k}$  events in all the other positions).

As far as the inclined tracks are concerned, four scans were performed with the GAMMA-400 module tilted by angles of  $15^\circ$ ,  $30^\circ$ ,  $45^\circ$  and  $60^\circ$ . Fig. 11 presents the spatial resolution results obtained in the different zones with respect to the tilt angle, considering only one implant width ( $60 \mu\text{m}$  for the  $120 \mu\text{m}$  strip zone and  $55 \mu\text{m}$  for the  $80 \mu\text{m}$  strip zone).

As documented in the literature [9], the spatial resolution shows a minimum around  $10^\circ$ , gradually deteriorating as the tilt angle is increased: at  $60^\circ$  the spatial resolution is worse than or equal to  $100 \mu\text{m}$  in every zone. For every tilt angle, the spatial resolution of the  $80 \mu\text{m}$  strip,  $240 \mu\text{m}$  readout is quite similar to the  $160 \mu\text{m}$  readout zone, with even slightly better results at large tilt angles.

## 5. Conclusions

The spatial resolution of a custom prototype of the silicon sensors for the converter-tracker of the GAMMA-400 experiment,

<sup>4</sup> CERN ROOT website: <http://root.cern.ch>

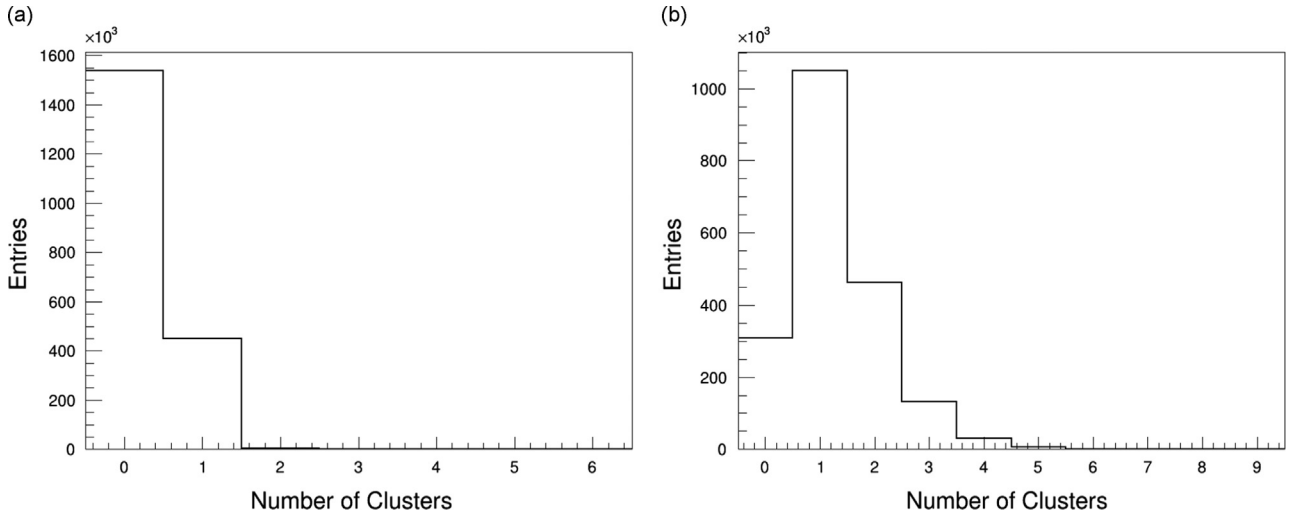


Fig. 7. Distribution of the number of clusters per event for the first beam telescope (a) and for the GAMMA-400 module (b).

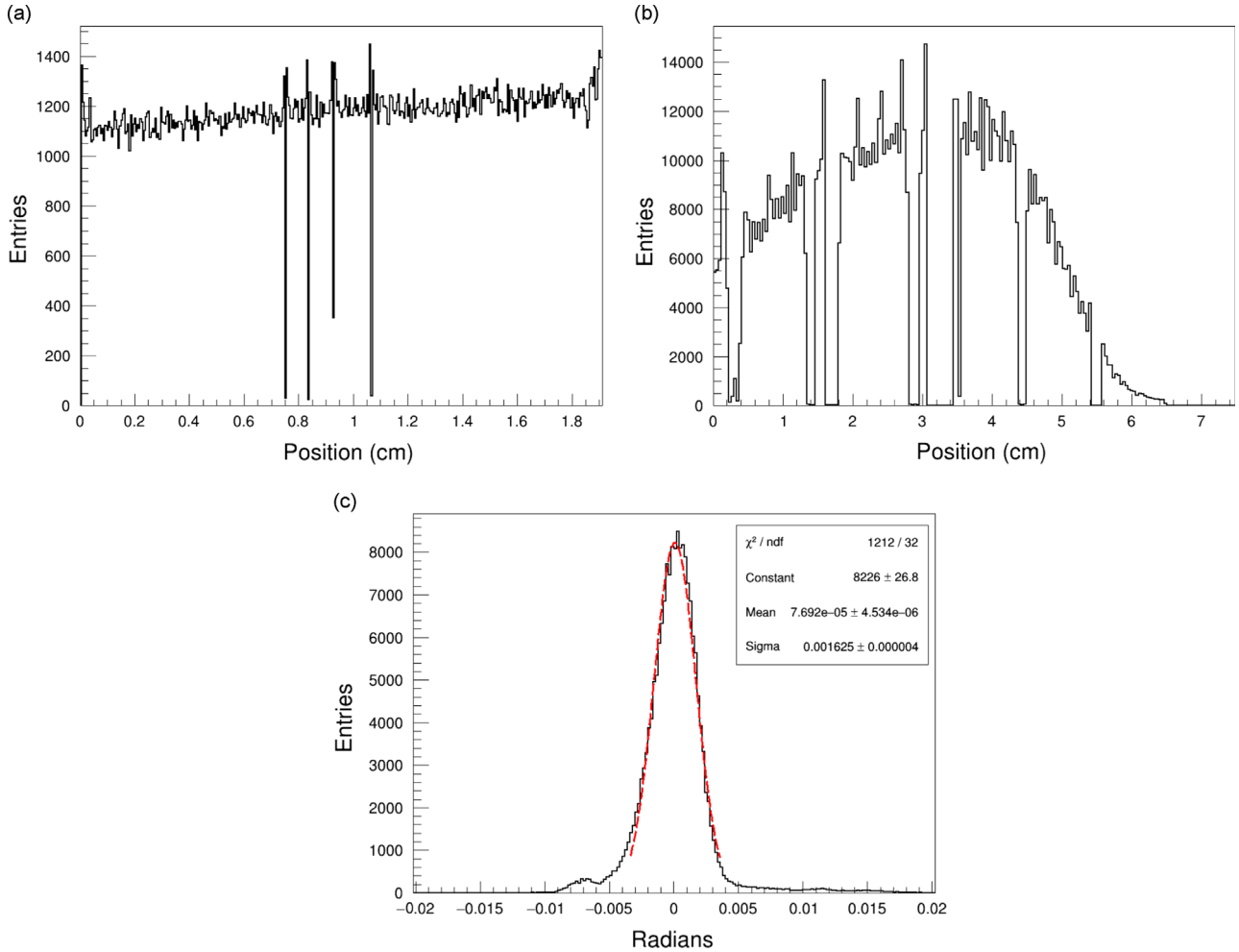
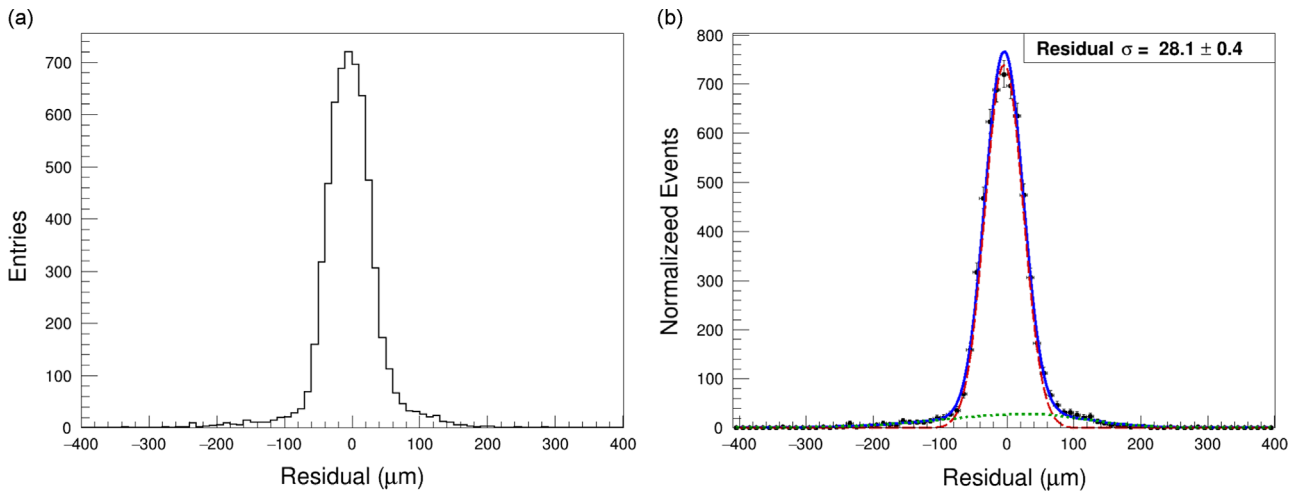


Fig. 8. Beam profile measured with the first beam telescope (a) and with the GAMMA-400 module (b); beam divergence of the T9 beamline (c).

characterized by different strip pitch, readout schemes and implant widths, was evaluated. The results show that the final readout scheme selected for the experiment, that is 80  $\mu\text{m}$  strip with a readout pitch of 240  $\mu\text{m}$ , guarantees optimal spatial

resolution measurements, with the advantage of a reduced number of readout channels. In particular, the spatial resolution obtained using the largest implant width is 28  $\mu\text{m}$  for non-inclined tracks, worsening up to 100  $\mu\text{m}$  for 60° inclined tracks.



**Fig. 9.** Residual distribution of the 80 μm strip, 240 μm readout pitch, 60 μm implant width zone (a) and the same distribution fitted with the composite Gaussian function (solid blue) (b); the simple Gaussian is drawn in dashed red, the asymmetric Gaussian in dotted green. (For interpretation of the references to color in this figure caption, the reader is referred to the web version of this paper.)

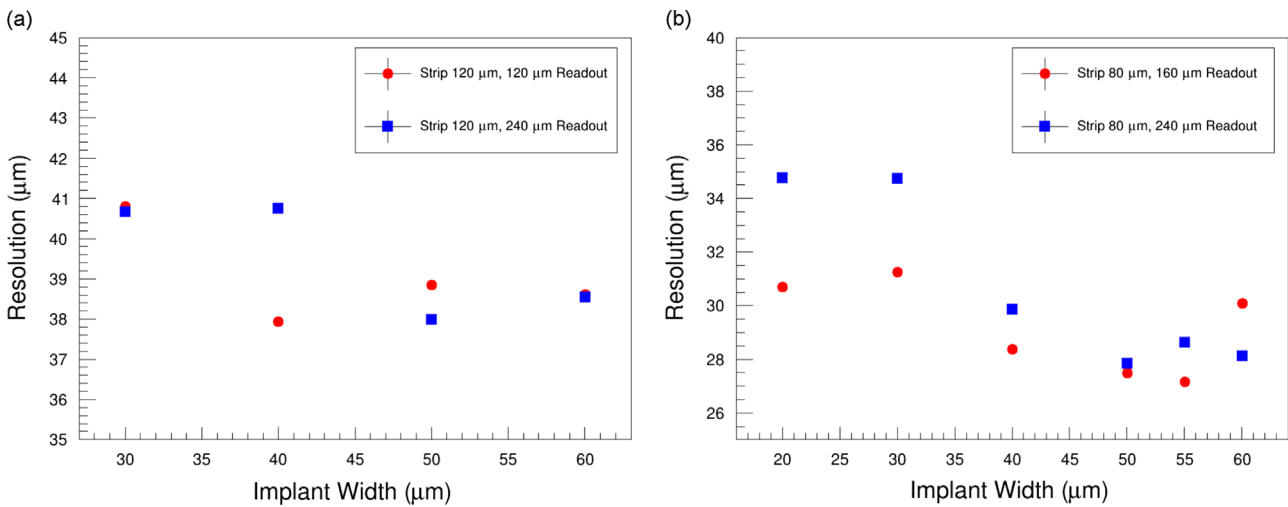


**Fig. 10.** Spatial resolutions obtained in the 120 μm strip zone (a) and in the 80 μm strip zone (b) as a function of the implant width for perpendicular tracks.

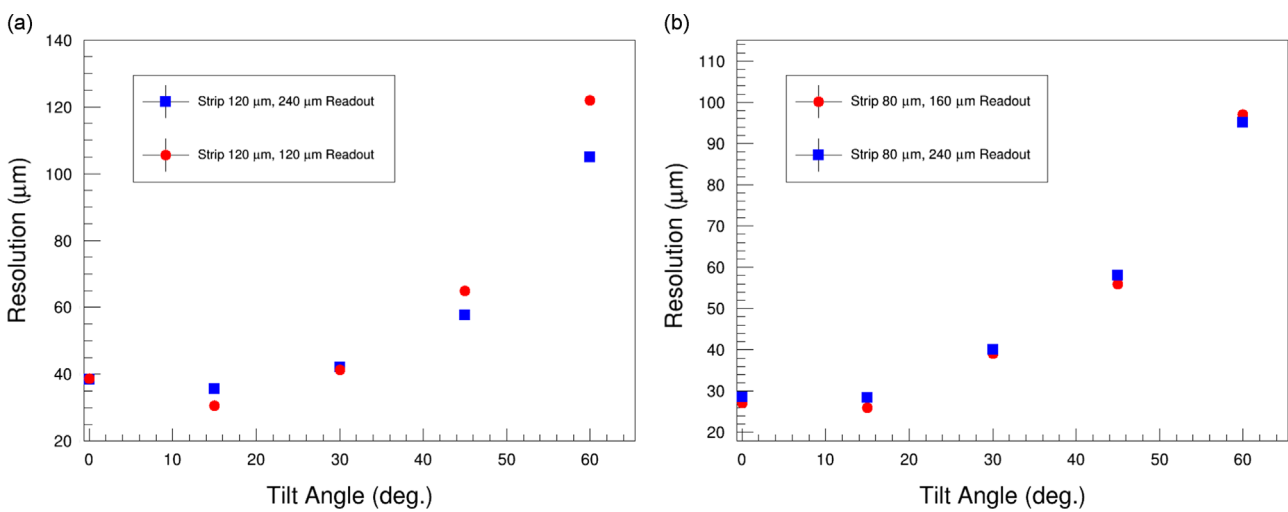


**Fig. 11.** Spatial resolutions obtained in the 120 μm strip zone (a) and in the 80 μm strip zone (b) as a function of the tilt angle.

## Acknowledgments

This work was supported by INFN. We would like to thank Giovanni Ambrosi, Maria Ionica, Andrea Nardinocchi and Vasile Postolache on INFN–Perugia for the help during the bonding phase of the GAMMA-400 silicon sensors and Maurizio Boscardin and Gabriele Giacomini of FBK for the support during the realization of the custom silicon sensors. We would also like to thank the PS staff, in particular Henric Wilkens and Lau Gatignon for the support during the data taking on the PS-T9 beamline.

## References

- [1] A.M. Galper, The GAMMA-400 space observatory: status and perspectives, in: Proceedings of SciNeGHE 2014, Lisbon, Portugal, [arXiv:1412.4239](https://arxiv.org/abs/1412.4239)[physics.ins-det].
- [2] P. Cumani, et al., The GAMMA-400 space mission, in: Proceedings of Fifth Fermi Symposium 2014, Nagoya, Japan, [arXiv:1502.02976](https://arxiv.org/abs/1502.02976)[astro-ph.IM].
- [3] U. Kotz, et al., Nuclear Instruments and Methods in Physics Research Section A 235 (1985) 481.
- [4] <http://cmm.fbk.eu/>.
- [5] Gamma Medica-Ideas, VA-140 Documentation, V0R1.
- [6] L. Celano, et al., Nuclear Instruments and Methods in Physics Research Section A 381 (1996) 49.
- [7] D. Lietti, et al., Nuclear Instruments and Methods in Physics Research Section A 729 (2013) 527.
- [8] A. Berra, et al., Nuclear Instruments and Methods in Physics Research Section A 735 (2014) 422.
- [9] R. Turchetta, Nuclear Instruments and Methods in Physics Research Section A 335 (1993) 44.